ADVANCED FUNCTIONAL MATERIALS
www.afm-journal.de

Versatile Agar-Zwitterion Hybrid Hydrogels for Temperature Self-Sensing and Electro-Responsive Actuation

Jueying Yang, Weiting Huang, Kelin Peng, Zhekun Cheng, Lizhi Lin, Jingjing Yuan, Yi Sun, Nam-Joon Cho, and Yu Chen**

Although recent years have seen considerable interest in stimuli-responsive hydrogels, their strict preparation conditions and narrow applicability limit their use as diverse sensors and soft robots. Herein, a versatile Agar-Zwirrions hybrid hydrogel actuator (Agar/PSBMA) integrated with simultaneous temperature self-sensing and wide-range electrical response is developed. To prepare the Agar/PSBMA hydrogel, a simple and controllable preforming post-enhancing and mechanical pressing method is used by introducing zwitterions materials into a temperature-sensitive Agar matrix. Owing to the design, the compact multiplex complementary structure generated by this method and the materials can facilitate the improvement of flexibility, stretchability, and toughness while providing mechanical dissipation and adhesion properties. Importantly, the visible detected temperature self-sensing ability during 10–40 °C, and quick and wide-range bending responses of both high-voltage and low-voltage electric fields make it unique over other actuators. Furthermore, the electrical response behavior of the hydrogel is found to be impacted by mechanical characteristics and charge polarization based on the finite element Abaqus simulations analysis. The prepared versatile hydrogels show the potential for applications as soft robotics and controlled transportation of adhered substances while simultaneously monitoring their working temperature, which expands the response range of hydrogel actuators and broadens the scope of application.

1. Introduction

As a class of intelligent polymers, hydrogel actuators can convert external stimuli,[1] such as pH,[2] light,[1] temperature,[3] magnetic,[4] and electric fields[5] into mechanical motion by shrinking, expanding, or bending. Among them, electro-responsive hydrogel actuators have received a lot of interest because of their low energy consumption,[6] quick response,[7] and accurate "on/off" process[8] under external electric field stimuli. Although current studies have demonstrated the large deformation[9] and quick motion modes[10] of electro-response hydrogels, most reports show strict preparation procedures and a narrow response range.

To improve the electro-responsive properties, ionizable groups are required in electro-responsive hydrogels that can provide a large number of fixed charges and respond quickly to electric fields.[11] Among them, zwitterion polymers exhibit a quick response to electric fields due to a large number of fixed charges and strong

J. Yang, W. Huang, K. Peng, J. Yuan, Y. Chen
School of Materials Science and Engineering
Beijing Institute of Technology
Beijing 100081, China
E-mail: bityuchen@bit.edu.cn

J. Yang, N.-J. Cho
School of Materials Science and Engineering
Nanyang Technological University
Singapore 639798, Singapore
E-mail: njcho@ntu.edu.sg

K. Peng
Yangtze Delta Region Academy of Beijing Institute of Technology
Jiaxing 314019, China

Z. Cheng
School of Aerospace Engineering
Beijing Institute of Technology
Beijing 100081, China

Z. Cheng
Department of Electrical and Computer Engineering
National University of Singapore
Singapore 119077, Singapore

L. Lin
Institute of Engineering Medicine
Beijing Institute of Technology
Beijing 10081, China

Y. Sun
Chinese Aeronautical Establishment
Beijing 100029, China

The ORCID identification number(s) for the author(s) of this article can be found under https://doi.org/10.1002/adfm.202313725

DOI: 10.1002/adfm.202313725

intermolecular dipole effects.[12] However, some challenges are associated with the preparation and application of these zwitterion hydrogels. Since the electro-responsive behaviors are related to the molecular weight and concentrations, the preparation conditions need to be strictly controlled during preparation.[13] In addition, most reported zwitterion hydrogels exhibit poor mechanical stability because of the irreversibly chemical cross-linking structure,[14] which limits their further applications.

Owing to their initiator-free preparation conditions and rigid polysaccharide structures, natural polymer Agar can be used as an ideal material to solve these problems. Agar is prone to form physically cross-linked structures via the simple heating-cooling process.[15] Due to hydrogen bonding between molecular chains, the preparation is no need for chemical cross-linking agents.[16] The polysaccharide structure of agar makes it highly mechanically stable and repeatable during the loading process. Moreover, it has been shown that Agar hydrogels allow the —OH group of the carbon backbone to interact with electrons, resulting in a structure with a net negative charge and bending in the electric field.[5] Therefore, Agar is appropriate for the controllable fabrication of green electro-responsive drives. However, Agar hydrogels are brittle in usage and have a restricted range of stretchability.

Herein, we develop versatile Agar-Zwitterions hybrid hydrogel actuators with temperature self-sensing and wide-range electro-response properties by introducing charge-rich sulfobetaine-based poly(sulfobetaine methacrylate) (PSBMA) to natural polymer Agar. A simple and controllable preforming post-enhancing method is applied via the physically cross-linked network of Agar, followed by the polymerization of SBMA to generate a post-enhanced double network hydrogel (Agar/PSBMA). By coupling with the mechanical pressing method, the multiplex complementary structure of the hybrid hydrogels may be beneficial for mechanical stability and adhesion ability. Together with the self-sensing and simultaneous response to both high and low-voltage electrical fields, the hybrid hydrogel is an ideal candidate as an intelligent pusher of the adhered items while providing the working temperature feedback.

2. Results and Discussion

2.1. Preparation of Agar/PSBMA Hydrogel

To solve the key issue in the strict preparation condition requirements and limited response range and variety exhibited by the majority of electro-responsive hydrogel actuators, Agar and SBMA were chosen in this work because of their self-supporting properties to easily prepare preformed hydrogel and the strong intermolecular dipole effects, which is beneficial for the electrical response. Versatile Agar/PSBMA double-network hydrogels were prepared by a simple and controllable preforming post-enhancing method combined with a mechanical pressing method, and the preparation mechanism is shown in **Figure 1**a.

SBMA is a typical zwitterionic polymer containing anionic and cationic groups, which can form a chemically cross-linked network via free radical polymerization. By mixing SBMA powders with the Agar solution at heating status, a mixed sol was poured into a mold (Figure S1, Supporting Information) or 3D printed (Figure S2 and Movie S1, Supporting Information) to create a preformed hydrogel with hydrogen bonding of Agar serving as the physical cross-linking point at low temperature. The physical cross-linking of Agar can uniformly disperse and support other reactive components, ensuring the uniform formation of the second network. The molding duration was controllably modified by altering the content of polymer components (Figure S3, Supporting Information). The free radical polymerization reaction of SBMA was triggered at 40 °C via the small molecule additives penetrating into the hydrogel network through solution penetration to create a second chemical cross-linking network and form Agar/PSBMA hydrogels. The elemental analysis of the edge and center part of Agar/PSBMA hydrogel indicated the sufficiency and uniformity of this cross-linking owing to the support the Agar to SBMA monomers (Figure S4, Supporting Information).

Using the preforming post-enhancing method, Agar/PSBMA hydrogel with the hybrid double network cross-linking network was constructed (Table S1, Supporting Information). Compared to the wrinkled and uneven surface of PSBMA hydrogel, Agar/PSBMA hydrogel showed a homogeneous structure (Figure 1b), indicating the second chemically cross-linked PSBMA network was well-distributed in the Agar substrate (Figure 1c). Furthermore, the preformed hydrogel cannot be prepared by the conventional method of adding reactants and additives in a solution system due to the organic additives disrupting the hydrogen bonding between Agar. Compared to the conventional method, the post-enhancing method using additive immersion avoided the direct contact between monomers and initiators in the solution system, making the hydrogel system with a uniform shape and higher degree of polymerization and thus showing an upper critical solution temperature (UCST) transition behavior of opaque at room temperature and the better mechanical properties (Figure S5, Supporting Information).

Moreover, after applying the mechanical pressing method, the hydrogel structure can be modified, and the cross-linking density is changed. The Agar/PSBMA can be enhanced by the mechanical pressing method by the following three steps. At first, the pressing force can cause the collapsed macropores of the Agar/PSBMA to increase the density of the cross-linked network. Then, the applied force makes it possible to break off the chemical bonds to generate the mechanoradical at the ends. Due to the physical network support, mechanoradical may trigger the polymerization of unreacted monomers or broken polymer chains, further improving the cross-linking density and mechanical properties. The mechanism of how the hydrogels are enhanced by the mechanical pressing method will be discussed further in the structure analysis and the mechanical property tests.

2.2. Composition and Morphological Characterization of Agar/PSBMA Hydrogel

The double cross-linking networks on the Agar/PSBMA hydrogels were investigated using ATR-FTIR, XPS, and SEM. The results of the ATR-FTIR tests are shown in **Figure 2**a. For SBMA and PSBMA, the decrease of the stretching vibrations of C=C at 1639 cm^{-1} indicated the polymerization of the SBMA monomers.[17] Agar/PSBMA hybrid hydrogels displayed both stretching vibration absorption peaks of —OH at 3436 cm^{-1} for Agar[18] and the characteristic peaks of S=O at 1032 and 1166 cm^{-1}, as well as C=O absorption peaks at 1717 cm^{-1} of

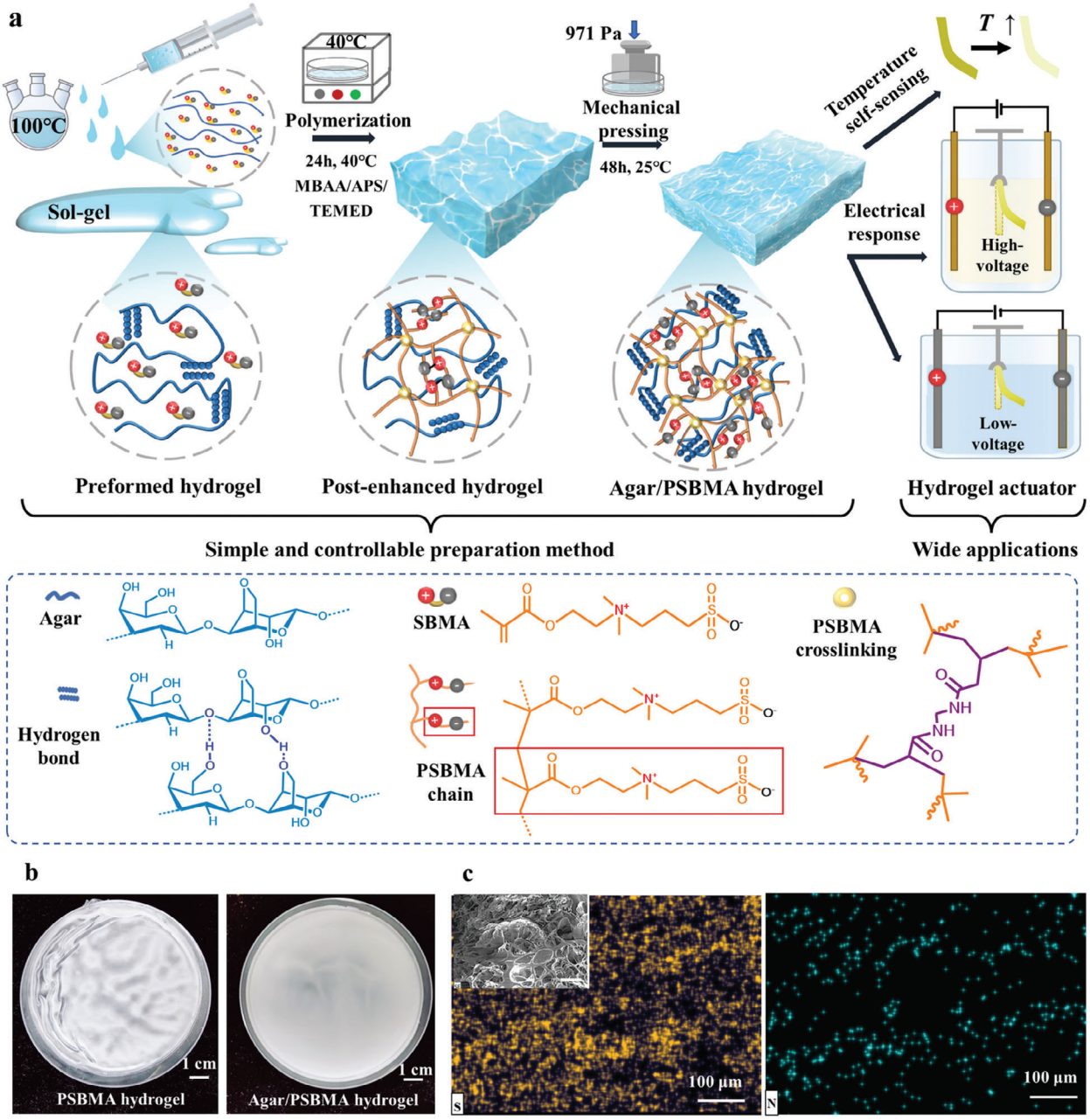

Figure 1. Synthesis of the Agar/PSBMA hydrogels. a) Schematic diagram and structural formula, including three steps of preforming, post-enhancing, and pressing. b) The appearance of PSBMA and Agar/PSBMA hydrogels. c) S and N element distribution in Agar/PSBMA hydrogel.

PSBMA,[19] indicating that the double network of Agar physical cross-linking and PABMA chemical cross-linking was formed in the hydrogel. In addition, the absorption peak of O—H in Agar moved to higher wavenumbers and the absorption peak of S=O moved to lower wavenumbers, indicating the smaller strength of hydrogen bonding resulted from the interaction between Agar and PSBMA and the decreased physical cross-linking.[20]

The XPS spectra of the preformed and the Agar/PSBMA hydrogels before and after the second chemical cross-linking network formation are shown in Figure 2b. In the high-resolution spectrum of N 1s in the preformed hydrogel, the main peak was the quaternary ammonium ion on SBMA ($-N^+R_4$, 401.9 eV), while the new peak in Agar/PSBMA hydrogel was the melamine group ($-NHR_2$, 400.9 eV). The high-resolution XPS spectra of C 1s in the preformed hydrogel correlate to the C—C (284.2 eV), —C—O/C—N (285.6 eV), and O—C—O/C=O (288.3 eV) peaks,[21] while a comparably substantial fraction of C—C peaks in the Agar/PSBMA hydrogel indicating more C—C bonds formed in the polymerization.

The comparison of the cross-sectional morphology of single network hydrogels and hybrid Agar/PSBMA hydrogels is shown in Figure 2c. Agar hydrogel exhibited hollow macropore and

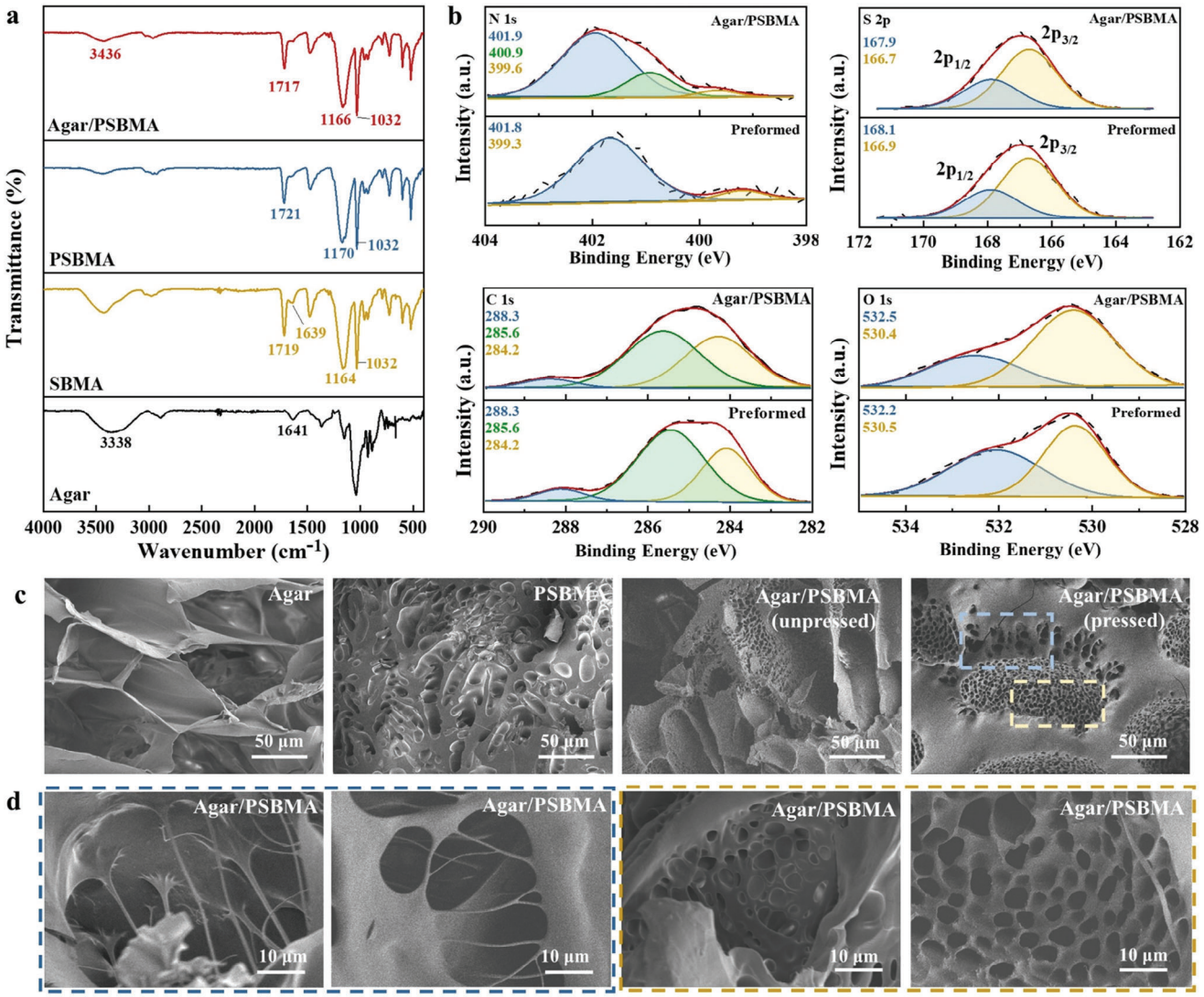

Figure 2. Structure and cross-sectional morphology of hydrogels. a) ATR-FTIR spectra. b) XPS spectra of preformed and Agar/PSBMA hydrogels. c) Cross-sectional morphology of single network and hybrid Agar/PSBMA hydrogels. d) SEM images of the compact multiplex complementary structure in Agar/PSBMA hydrogels.

lamellar structures with a pore diameter of >100 μm, indicating the brittle physically cross-linked network.[22] PSBMA presented a compact well-distributed micropore structure because of the uniform chemically cross-linked network, with the pore diameter ≈15 μm. Interestingly, in the hybrid Agar/PSBMA hydrogels, the hierarchical pattern of large pores containing small pores was found regardless of whether the hydrogel has been mechanically pressed and toughened. The hybrid structure was identified by macropores from Agar physical cross-linking and micropores from PSBMA chemical cross-linking networks. As a result of mechanical pressing, the Agar/PSBMA hydrogel exhibited a compact multiplex complementary structure with collapsed macropores shown in Figure 2c,d. In the multiplex complementary structure, filamentary or smaller pore linkages appeared within the pores of the hydrogel. Since the S and N elements in the hydrogel are primarily derived from SBMA, the elemental distribution diagram of the hydrogel revealed that the filament or small pores in the hydrogel are primarily derived from the cross-linked chemical network (Figure S4, Supporting Information).[23] The reason for the formation of the multiplex complementary structure may be that pressing force can promote the aggregation of reactants in large pores under the support of the Agar network, making the cross-linking network formed more concentrated. The compact multiplex complementary structure can facilitate the improvement of hydrogel toughness, provide mechanical dissipation, and enhance the swelling resistance of Agar/PSBMA hydrogel,[24] enabling it to maintain structural stability in water for a long time (Figure S6, Supporting Information).

2.3. Mechanical and Adhesion Properties

The formation of the double network had a toughening effect on the hydrogel, and hydrogels containing >1%

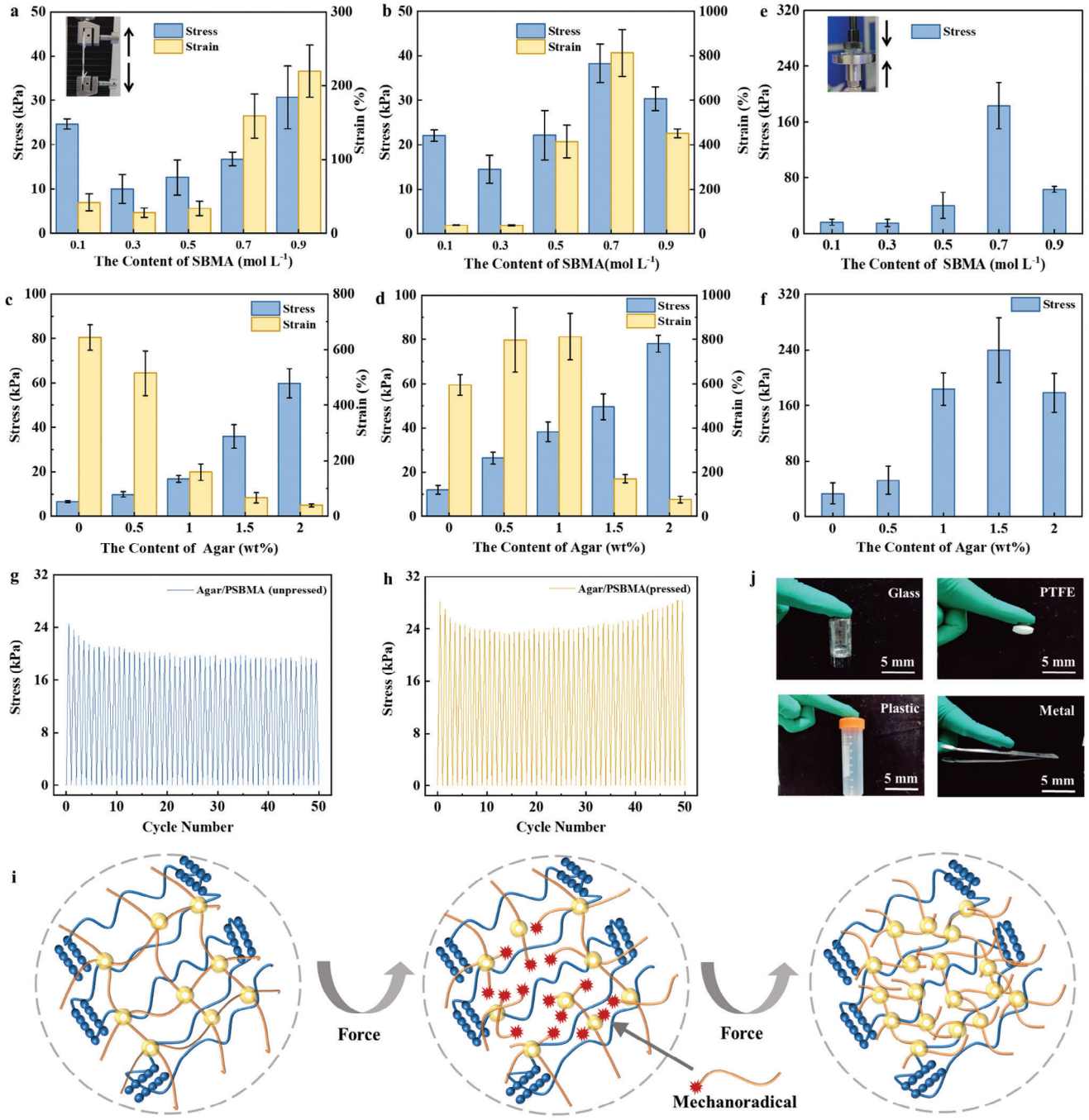

Figure 3. Mechanical tests of Agar/PSBMA hydrogels. a,b) Tensile tests of hydrogels with different SBMA contents before (a) and after (b) compression. c,d) Tensile tests of hydrogels with different Agar contents before (c) and after (d) compression. e,f) Compression tests of hydrogel with different SBMA contents (e) and different Agar contents (f). g,h) Mechanical cycling test of Agar/PSBMA hydrogels before (g) and after (h) pressing. i) The mechanism of mechanical pressing enhancement and the adherence. j) Adhesion of hydrogels to polar and non-polar surfaces.

Agar or >0.5 mol L^{-1} PSBMA were capable of deforming from complex-shaped molds with minimal shape damage (Figure S1, Supporting Information). The mechanical properties of Agar/PSBMA hydrogels with different PSBMA contents are shown in **Figure** 3a,b. The tensile strength and elongation decreased at first and then increased with higher PSBMA content. This is because the steric and zwitterionic effects caused by the addition of PSBMA influenced the development of hydrogen bonds between Agar, resulting in a decrease in tensile properties. As the PSBMA content increased, the newly generated chemically cross-linked network made up for the impact of hydrogen bond reduction on the mechanical properties and gradually occupied a dominant position in the contribution to the tensile properties, increasing in the

tensile strength and elongation. The mechanical properties of Agar/PSBMA hydrogels with different Agar contents are shown in Figure 3c,d. The tensile strength of Agar/PSBMA hydrogels increased and the elongation decreased as the Agar content rose because the physically cross-linked network enhanced the mechanical strength of hydrogels. As tensile distance increased, the hydrogen bonds in Agar were more easily broken, limiting the gain in fracture elongation. For the compression test shown in Figure 3e,f, higher PSBMA content increased the density of the chemical cross-linked network and higher Agar content enhanced the density of the hydrogen bonding network in the system, improving the mechanical dissipation of the hydrogel and thus its resistance to compression. However, when the content of one component is too high, the hydrogel tends to exhibit a single-network behavior and loses its mechanical dissipation effect,[25] thus limiting the improvement of compressive stress. From the mechanical tensile curves, the Agar/PSBMA hydrogel exhibited the characteristics of a double-network hydrogel, where physical and chemical networks worked in conjunction to provide strength and toughness.

In addition, the mechanically pressed hydrogels had a significant increase in tensile strength and elongation at break. Pressed Agar/PSBMA hydrogels exhibited an increase both in the stress and the elongation with the pressing force increased (Figure S7, Supporting Information). The Agar/PSBMA hydrogel after pressed exhibited an elongation of 812.5% while maintaining a tensile stress of 47.3 kPa. According to the integrated area of the stress-displacement curve, the fracture energy of Agar/PSBMA hydrogel after pressing reached 5740 $J \cdot m^{-2}$, which is 11 times that of the hydrogel before being pressed (Table S2, Supporting Information). The results of tensile and compression cycling tests are shown in Figure 3g,h and Movies S2 and S3 (Supporting Information). Agar/PSBMA hydrogel before mechanically pressed retained 68% tensile strength after 50 loading-unloading cycles, while Agar/PSBMA hydrogel after pressed retained 100% tensile strength after 50 loading-unloading cycles, indicating that mechanical pressing has a strengthening effect and excellent fatigue resistance capabilities.

The reasons for the mechanical pressing enhancement can be attributed to force-triggered chemical reactions.[26] In Agar/PSBMA hydrogel, the force applied to the physical/chemical hybrid double network easily led to the chemical bonds of the PSBMA network breaking, generating a large number of mechanoradical at the ends (Figure 3i). Due to the physical network support and regional suppression of Agar, mechanoradical may be concentrated in certain regions and trigger the polymerization of monomers or broken polymer chains, further improving the mechanical properties. The cross-linking density of the hydrogel has been improved after mechanical pressing was also proved by the swelling ratio and the rheological tests.[22,24] Compared with the swelling ratio of the hydrogel before pressing, the swelling ratio of the hydrogel after pressing was lower or similar (Figure S6, Supporting Information), indicating the mechanical pressing can increase the cross-linking density inside the hydrogels. The storage modulus and loss modulus after the mechanical pressing is much higher than that of the hydrogels before mechanical pressing as shown in the following figure, which also indicates the cross-linking density of the hydrogel after mechanical pressing has been improved (Figure S8, Supporting Information). This result can also be observed through the multiplex complementary structure in Figure 2. Mechanical pressing increased the density of the PSBMA chemically cross-linked network and the connection structure between large pores. These multiplex complementary structures provided superior mechanical dissipation and thus improved the tensile properties of hydrogels with the physical/chemical hybrid double network.

The mechanoradical introduced by mechanical pressing method can also promote the adhesive properties of the Agar/PSBMA hydrogel. The adhesion cycles were performed via repeatedly peeling and contacting the hydrogel with the attached object and mechanically pressed. The adhesion energy was estimated from the curved area of adhesion strength and displacement. The hydrogels demonstrated steadily increased adhesion behavior as the duration of applying a pressing force on the hydrogels was extended (Figure S9, Supporting Information). After 4 days of pressing, the adhesion energy of the hydrogel to rubber and metal increased by 8.9 and 8.0 times, respectively, to 61.4 and 41.5 $J\ m^{-2}$. The increase in adhesion energy was attributed to hydrogen bonding and dipole–dipole interaction.[27] The mechanical interlocking interaction with the surface of the attached object may occur by the mechanoradical generated by the pressing force to improve the adhesion performance of hydrogels. With the increase of the pressing time, the surface roughness of the hydrogel increases, and the mechanical interlock with the surface of the adhered object increases, so the adhesion energy is further improved. The adhesion properties of Agar/PSBMA hydrogels to polar and non-polar object surfaces, including glass, Teflon, plastic, and metal are shown in Figure 3j. The proper adhesion properties of Agar/PSBMA hydrogel make it possible to control the movement of adherent objects according to external stimuli.

2.4. Temperature Self-Sensing

In addition to the ability to respond to external stimuli, it can further broaden the application scenarios of hydrogels if the actuator itself has sensing performance that is identifiable by the eye. Owing to the UCST behaviors by strong intramolecular and intermolecular electrostatic interactions between zwitterionic groups of PSBMA polymers,[28] it may enable the temperature self-sensing of Agar/PSBMA hydrogels. The thermally responsive optical behavior of Agar/PSBMA hydrogel was characterized by the transparency changes during the wide temperature range of 10–40 °C (**Figure 4**). This self-sensing ability is achieved by the material itself, without the need for other sensing devices.

The temperature self-sensing of Agar/PSBMA hydrogel is related to the component content. As shown in Figure 4a, the transparency of Agar/PSBMA hydrogel below the UCST was affected by the SBMA content. When the SBMA content was 0.5 mol L^{-1}, the UCST behavior could hardly be differentiated by eyes, showing that the UCST temperature was related to the content of SBMA and it increased rapidly as the content increased at low concentrations while reaching a stable level at high concentrations.[29] The transparency of Agar/PSBMA hydrogel above UCST is affected by the Agar content. The higher the Agar content, the lower the transparency of the hydrogel.

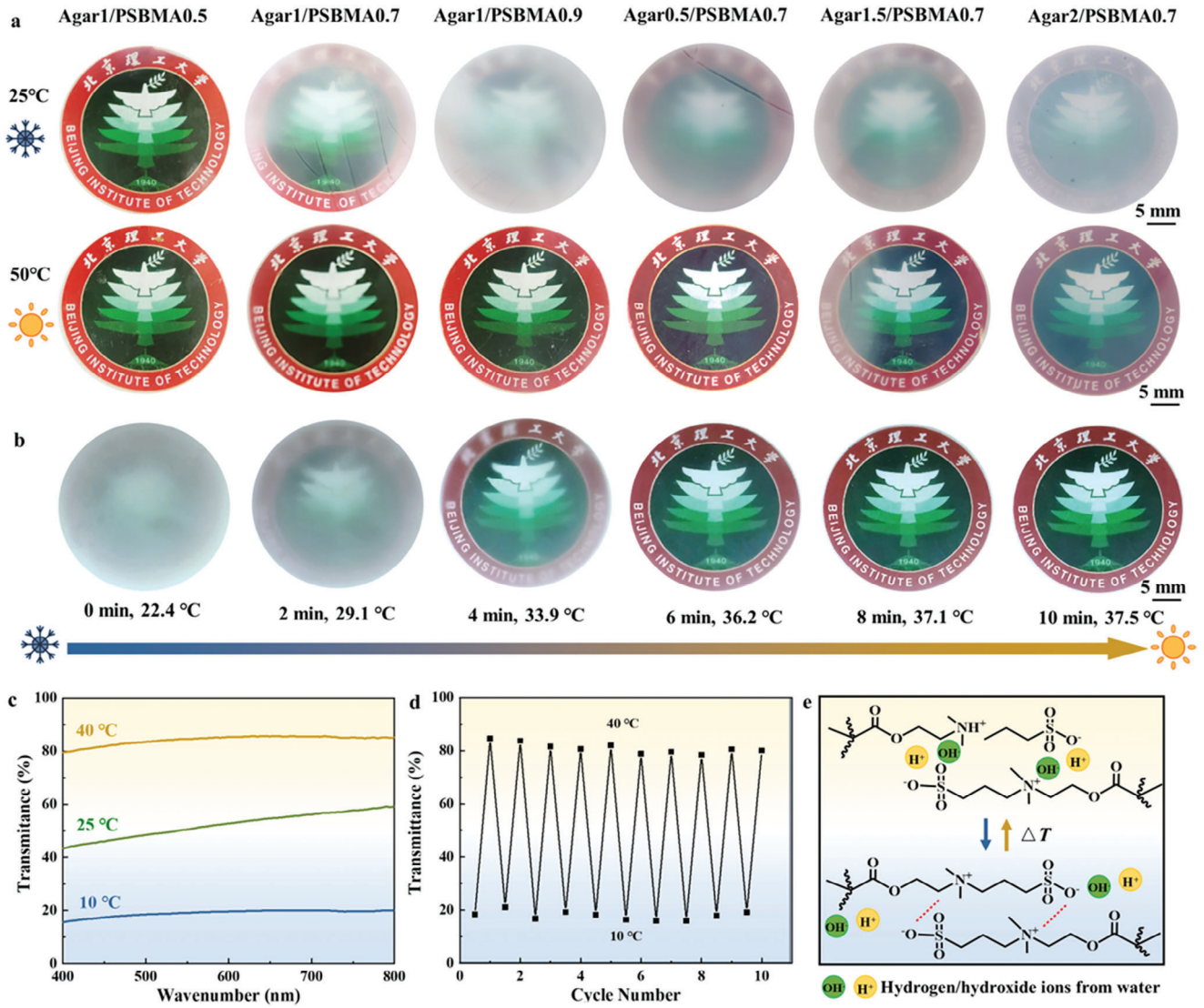

Figure 4. Temperature self-sensing properties of Agar/PSBMA hydrogels. a) The transparency changes of Agar/PSBMA hydrogels with different SBMA and Agar contents under and above the UCST temperature. b) The transparency changes of Agar/PSBMA hydrogels as the temperature increased. c) The transmittance of Agar/PSBMA hydrogels under different temperature at 550 nm wavelength. d) The transmittance of Agar/PSBMA hydrogels during different temperature cycles. e) Schematic diagram of temperature self-sensing mechanism.

The UCST behaviors of Agar/PSBMA hydrogel can be characterized quantitively by the change in optical transparency under different temperatures at the SBMA content of 0.7 mol L^{-1}.[30] As shown in Figure 4b, when the temperature rose from room temperature to 37.5 °C, the hydrogel gradually changed from opaque to transparent, showing obvious UCST behavior. Quantitative characterization of the changes in Agar/PSBMA transparency through UV–vis spectroscopy showed that the transmittance of the hydrogel increased significantly with increasing temperature (Figure 4c). This change in transparency was reversible and can still maintain the UCST behavior after ten times switching of high and low temperatures (Figure 4d),[31] indicating that its temperature self-sensing characteristics were durable and repeatable.

The mechanism of the temperature self-sensing behavior of Agar/PSBMA can be explained by the dipole–dipole interaction and electrostatic interaction between oppositely charged ionic groups (Figure 4e).[32] Since PSBMA carries both positive and negative charges, inter- and intra-chain electrostatic interactions are formed below UCST, exhibiting opaque properties due to phase separation. When it is heated above UCST, the electrostatic self-association between zwitterionic chains is overcome, and water molecules are inserted between the chains, making the disordered structure and the solubility of PSBMA in water, so it appears optically transparent macroscopically.[33] These self-sensing properties bring Agar/PSBMA hydrogels the possibility of application as monitoring the working temperature for actuators.

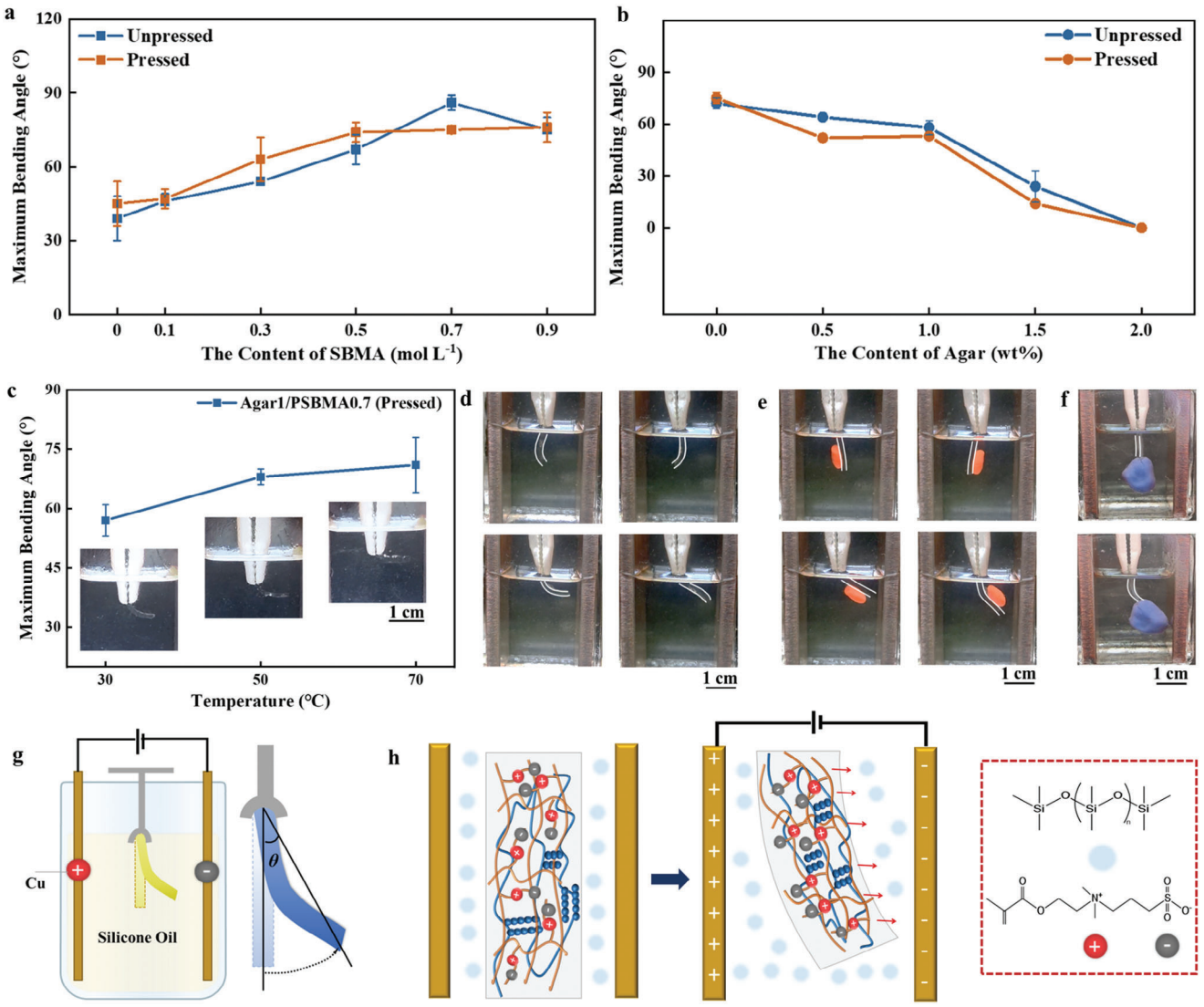

Figure 5. High-voltage electrical response performance tests of hydrogels. a,b) High-voltage electrical response performance of hydrogels with different PSBMA contents (a) and different Agar contents (b). c) Effect of temperature on the high-voltage electrical response performance of Agar/PSBMA hydrogels and their corresponding working temperature feedback. d) Electrical response of the same hydrogel with different initial orientations. e) Electrical response of objects adhered to different sides of the same hydrogel. f) Locomotion of an object adhering to the hydrogel. g) Schematic diagram of high-voltage electrical response performance test. h) Mechanism of high-voltage electrical response performance.

2.5. Electrical Response Performance

To investigate the high-voltage electrical response of Agar/PSBMA hydrogel, a test platform was constructed for recording and measuring the maximum bending angle of these actuators (Movie S4, Supporting Information). **Figure** 5a,b illustrates the influences of component content and mechanical pressing on the electrical response of hydrogel actuators. The maximum bending angle of the hydrogel rose with increasing PSBMA content and decreased with increasing Agar content. The increase in PSBMA proportion decreased the elastic modulus of hydrogel, therefore enhancing its deformation degree (Table S2, Supporting Information). Its strong dipole–dipole interaction increases the number of movable ions within the Agar/PSBMA hydrogel, which improves its electrical responsiveness, thereby increasing its maximum bending angle to 86° within 1 s (Figure S10, Supporting Information). Additionally, an increase in the Agar proportion results in a decrease in toughness and a decrease in the deformability of Agar/PSBMA hydrogel. Mechanical pressing did not affect the electro-responsiveness of the hydrogel even though a force-triggered multiplex complementary structure was formed. It indicates that the deformation of the hydrogel is closely related to its charge distribution of polymer chains, not its microstructure. In addition, the mechanical pressing method ensures that the hydrogel is not easily broken during cyclic actuating. During three cycles, the standard deviation of the maximum bending angle was ± 3.2°, further demonstrating that the toughness of the hydrogel can ensure the cyclic robustness of the hydrogel (Figure S11, Supporting Information).

Figure 5c shows the effect of temperature on the electrical response performance. An increase in temperature results in a greater maximum bending angle. This is a result of the molecular movements inside the hydrogel becoming faster and more flexible due to the increase in temperature. In addition, due to the temperature self-sensing property, Agar/PSBMA hydrogel can also be used as a working temperature indicator, changing from opaque to transparent when the temperature increases (insert images of Figure 5c). These temperature self-sensing properties make it possible to alarm when the working environment is hot, thus avoiding the direct touch and ensuring immediate detection when the temperature rises abnormally.

Certain applications of hydrogel actuators were investigated in this study. Since the Agar/PSBMA hydrogel exhibits a uniform structure, its bending direction is not affected by the initial orientation (Figure 5d). This brings the possibility of hydrogels being used as smart putters. It can be seen from Figure 5e that no matter which side of the hydrogel the object is adhered to, the bending direction of the hydrogel will not change, indicating that the electrical response behavior of the hydrogel is not affected by the adhered object.[34] However, the maximum bending angle of the hydrogel actuator after adhering to an object can reach 62°, which is slightly smaller than the maximum bending angle (72°) without adhering to an object. This is because the mass of the hydrogel actuator after adhering to an object becomes larger, which will reduce the bending angle to a certain extent. In addition, objects ten times the weight of Agar/PSBMA hydrogel were also capable of being adhered and carried to move in the direction of the electrode (Figure 5f; Movie S5, Supporting Information). Therefore, this actuator has the potential to be used as an intelligent pusher to control the propulsive transport of adhered objects.

The electrical response mechanism of Agar/PSBMA under a high-voltage electric field can be divided into three stages (Figure 5g,h). Initially, a non-uniform electric field effect is produced between parallel plate electrodes when a high-voltage electric field is applied. Then, the positively and negatively charged groups on PSBMA are oriented and arranged under the electric field, and the asymmetric dipoles in the Agar structure become polarized. As a result, the dipole moment increases and a dielectrophoretic force is produced. Lastly, because the top of the hydrogel is fixed, the attractive forces produced between the electrodes and the charged groups of the free-oscillating bottom component cause the hydrogel to bend in reaction to the electric field. It can be inferred that the polarization and dipole moment within the polymers affects the bending angle. This was also proven with hydrogels prepared by Agar and different polymers (Figure S12, Supporting Information). Since the number of charges contained in the repeating units of zwitterions is higher than that of polyanions and polycations, Agar/PSBMA hydrogel showed the largest bending angle compared to Agar, Agar/sodium alginate (SA), and Agar/chitosan (CTS). The bending direction is affected by the non-uniform electric field effect produced between parallel plate electrodes. Hydrogels tend to bend toward electrodes that are farther away from them (Figure S13, Supporting Information). In an ideal state, the hydrogel will not bend when located in the middle of the electrode because the electrode action counteracts each other. However, the position of the hydrogel will always shift to a certain extent in reality, so the hydrogel will bend toward one of the electrodes.

To investigate the low-voltage electrical response of Agar/PSBMA hydrogel, a designed low-voltage electrical platform was used in this study in 0.1 mol L^{-1} Na_2SO_4 solution. **Figure 6**,b demonstrates that the maximum bending angle of the hydrogel is positively correlated with the PSBMA content, and inversely related to the Agar content. This phenomenon can be attributed to the decline in the modulus of the hydrogel actuator, which occurs concomitantly with an increase in the proportion of PSBMA content or a decrease in the percentage of Agar content. Electric field strength has an impact on the low voltage electrical response of Agar/PSBMA hydrogel (Figure 6c), which exhibited the highest bending angle of 55° within 30 min at a low voltage of 15 V. The increase in voltage can increase the maximum bending angle and response speed of the hydrogel actuator. Furthermore, the Agar/PSBMA hydrogel exhibited environmental stability in both acid and alkali solutions (Figure 6d). In the water environment without ions, hydrogels would not respond to the low-voltage electric field.

According to the theory of classical electro-responsive systems, the bending of the actuators is owing to asymmetric swelling caused by osmotic pressure difference,[35] which is produced by the movement of the counterbalance ion of the polyelectrolytes toward the counterbalance electrode while the polyions of the hydrogel network remain immobile.[36] It was found that when the PSBMA content is >0.5 mol L^{-1}, the zwitterion hydrogel can also bend at low electric fields. The mechanism of stimuli-response behavior was studied. First, the free ions in the dielectric Na_2SO_4 solution undergo an electrolytic interaction with the water when an electric field is introduced, and then they migrate toward the balancing electrode. Second, the volume of cations in the PSBMA polymer network is smaller than that of anions and moves faster toward the cathode, resulting in the osmotic pressure of the hydrogel near the anode greater than that near the cathode.[8,37] The bending direction is affected by different ion mobility rates. Finally, an osmotic pressure difference between the two sides of the hydrogel appeared. One side with larger osmotic pressure expands while the other with less osmotic pressure contracts to generate the bending behavior toward the cathode. As time goes on, the osmotic pressure difference between the two sides will steadily rise. The bending angle of the hydrogel achieves its maximum value and is unaffected after the osmotic pressure approaches dynamic equilibrium (Figure 6e,f). Since there are very few mobile ions in pure water, a large osmotic pressure difference cannot be generated, and the hydrogel does not show obvious bending changes.

Consequently, responding to high-voltage and low-voltage electric fields simultaneously requires hydrogels to be polarizable and have a certain amount of ion mobility.[38] It is the polarizable asymmetric ion-dipole moment within the Agar, the strong dipole–dipole interaction in PSBMA, as well as the induced ion polarization that renders the bending of hydrogel actuators at high voltage.[24] Under low voltage, the hydrogel bends due to osmotic pressure differences brought about by the migration of zwitterions in PSBMA. As a result, zwitterions in PSBMA produce large molecular dipoles and cause polarization of the Agar, while the zwitterions can move in response to the applied electric field, which results in Agar/PSBMA hydrogel response to both high-voltage and low-voltage electric fields simultaneously.

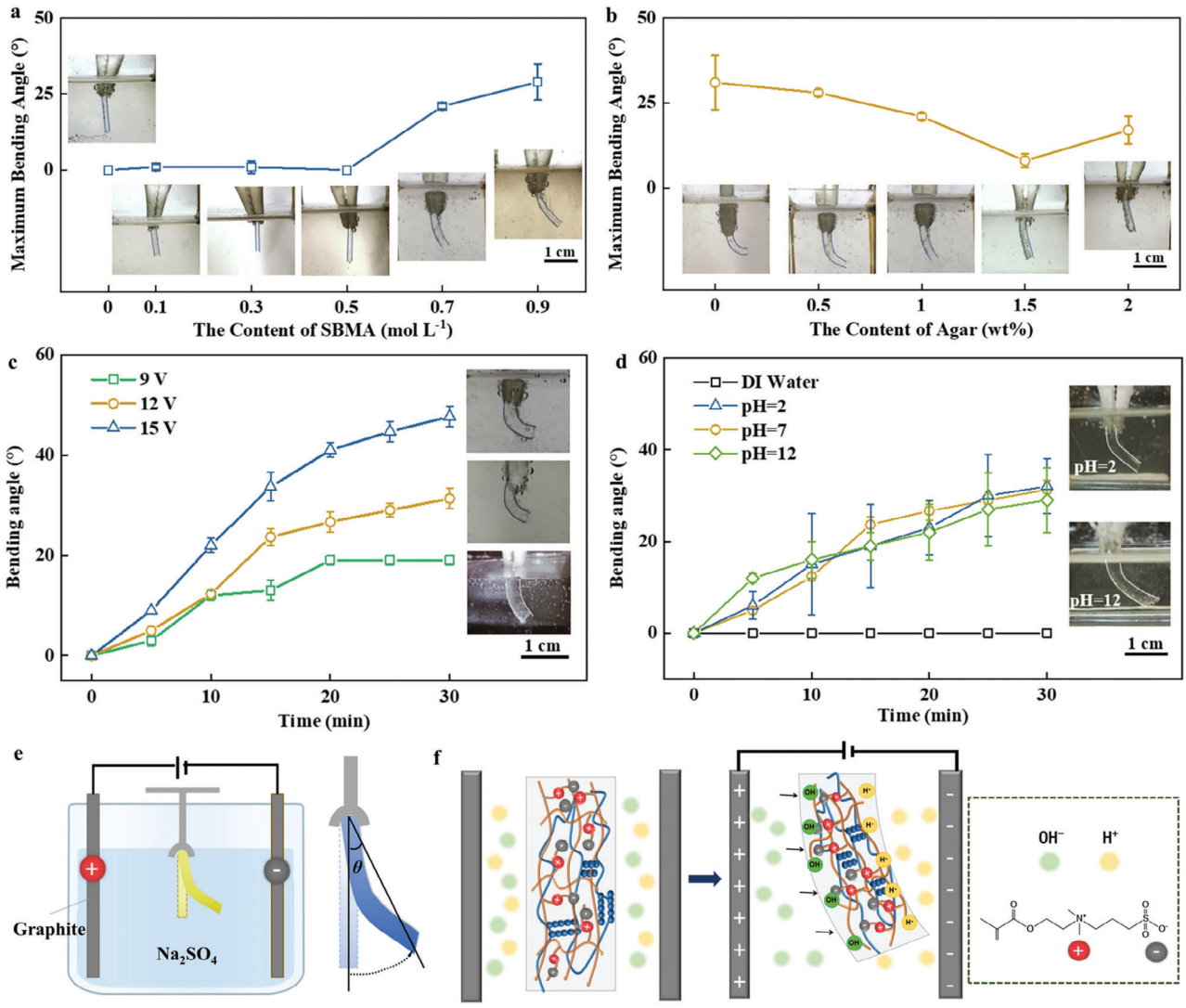

Figure 6. Low-voltage electrical response performance test of hydrogels. a,b) Low-voltage electrical response performance of hydrogels with different PSBMA contents (a) and different Agar contents (b). c) Effect of voltage on the low-voltage electrical response performance of Agar/PSBMA hydrogels. d) Effect of solution pH on the low-voltage electrical response performance of Agar/PSBMA hydrogels. e) Schematic diagram of low-voltage electrical response performance test. f) Principle of low-voltage electrical response performance.

Compared with typical hydrogel actuators in other relevant studies (**Table 1**), the key advance of the hydrogels is that the Agar/PSBMA hydrogel exhibits simultaneous temperature self-sensing and wide-range electrical responsiveness, which has the potential for electrical response applications as soft robotics while simultaneously monitoring their working temperature. In addition, the pressing force-triggered hybrid Agar/PSBMA hydrogel shows soft mechanical strength yet long elongation, which can meet the application requirements of actuators. The hybrid Agar/PSBMA hydrogel contained zwitterion polymers and natural polymer Agar, bringing the possibility of temperature self-sensing of the hydrogels compared with natural materials[5,9,39] and maintaining sustainability compared with other synthetic polymers.[8,10,40] Therefore, the temperature self-sensing and wide-range electro-response properties of the Agar/PSBMA hydrogels make it a unique prospect over other actuators.

2.6. The Influence Factors and Regulations of the Electrical Response

To analyze the interaction among hydrogel structure, conductivity, dielectric constant, and their electrical response properties, the electrochemical properties of the hydrogels were examined using an electrochemical workstation and an LCR meter (**Figure 7**). As observed from Figure 7a,b, PSBMA content increase leads to a rise in the number of ionizable ions and polarization rate, as well as enhanced electrical conductivity.[41] PSBMA hydrogel network containing zwitterions exhibits synergistic dipole arrangement, leading to a significant increase in the dielectric constant and bending angle under the electric field. This is consistent with the electrical response results shown in Figures 5 and 6. Hence, it is inferred that electrical properties within the hydrogel are one of the factors influencing the electrical response

Table 1. The studies of actuators with maximum bending angle under external stimuli.

Materials	Stress [kPa]	Strain [%]	Self-sensing	Maximum bending angle	Reference
CTS/carboxymethyl cellulose film	-	-	-	90° under low-voltage electric field	[9]
Agarose hydrogel	-	-	-	75° under high-voltage electric filed	[5]
Bamboo/poly(N-isopropylacrylamide) hydrogel	5300 (parallel) and 47 (perpendicular)	2 and 10	-	45°–360° under NIR light	[39a]
Carboxymethyl cellulose/gelatin/SA hydrogel	-	-	pH	≈80° under low-voltage electric field	[39b]
Poly(acrylic acid) with $Al(OH)_3$ nanoparticles	1958.7	744	-	≈50° under low-voltage electric filed	[8]
K-MXene/PEDOT:PSS with poly(N-isopropylacrylamide) hydrogels	≈12	≈560	Strain	50° under 808 nm NIR light	[10]
P(2-acrylamido-2-methyl-1-propanesulfonic acid-co-acrylic acid)-based composite hydrogel	407	≈100	-	90° under low-voltage electric field	[40a]
Hard magnetorheological elastomers	≈200	15	Mechanical loading	≈33° under magnetic field	[40b]
Polyvinyl chloride gel	26.4	≈170	-	82° under high-voltage electric filed	[40c]
Poly(acrylic acid)/polypyrrole hydrogel	≈250	25	-	22° under low-voltage electric filed	[40d]
Agar/PSBMA hydrogel	47.3	812.5	Temperature	86°/55° under high-voltage/low-voltage electric filed	This work

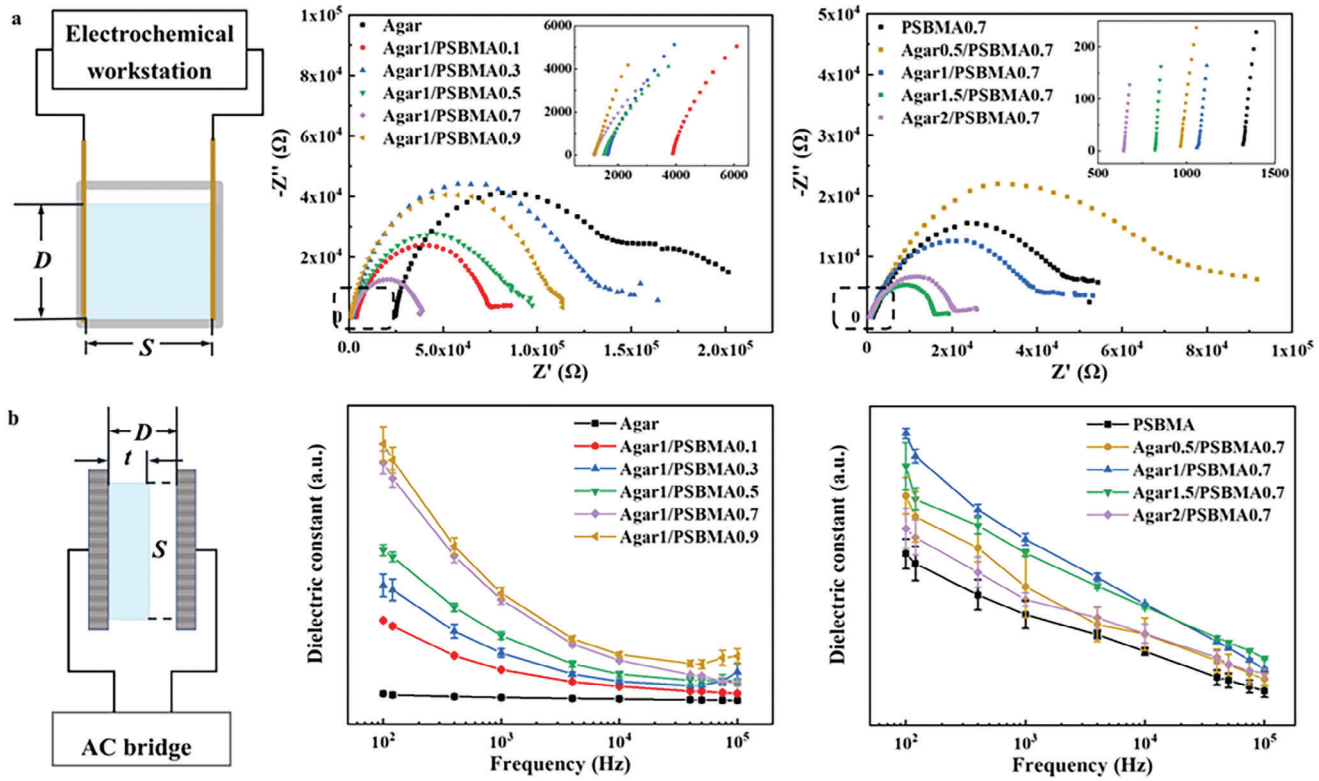

Figure 7. Electrical properties of hydrogels. a) Conductivity of hydrogels with different polymer contents (insert images: enlargement of the data near Z' = 0). b) Capacitance of hydrogels with different polymer contents.

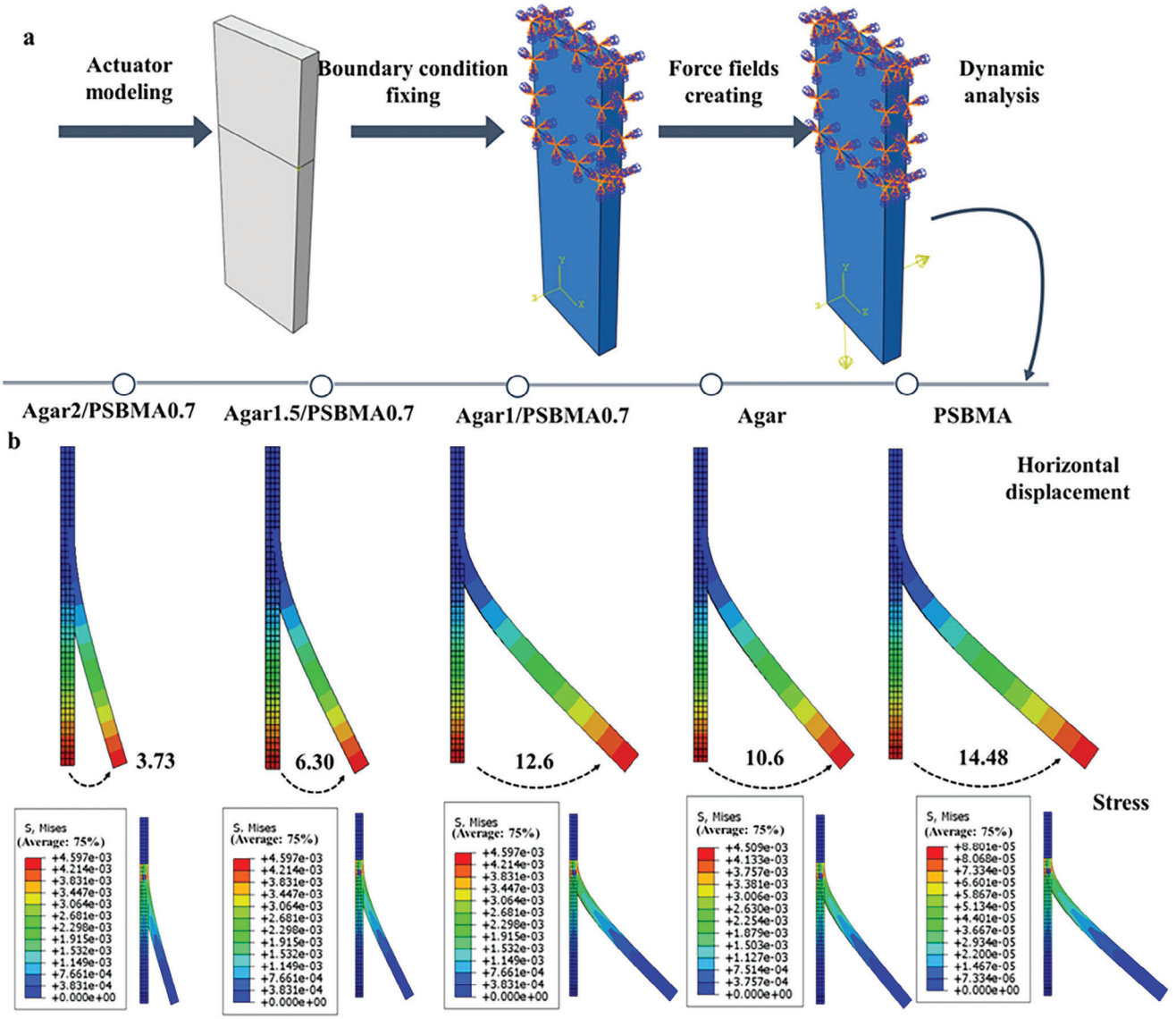

Figure 8. Force-electric coupling results. a) Force-electric coupling process. b) Force-electric coupling results of different component hydrogel drives, where S represents the stress change in the hydrogel.

behavior. On the one hand, the electrical response of Agar/PSBMA hydrogels results from the difference in ion distribution. With the basis of ion movement, the increased ion diffusion leads to enhanced electrical conductivity and responsiveness.[42] On the other hand, the application of actuators requires high dielectric constants because an increase in dielectric constant reduces the Coulomb electrostatic interaction energy between charged substances and facilitates ion transport.[43] The higher the dielectric constant means the more polarizable the hydrogel under the applied electric field. Therefore, strong dipole-dipole interactions, high ion density, and fast ion dissociation and migration can significantly enhance the bending strain of hydrogel actuators when viewed from the perspective of electrical properties.[44]

Figure 7 indicates that increasing Agar content results in higher conductivity and dielectric constant due to the introduction of more polarizable molecular chains. However, Figures 5 and 6 demonstrate that increasing Agar content reduces the bending angle, suggesting that the electrical response behavior of the hydrogel is regulated not only by its electrical properties but also by its mechanical properties.[45] To demonstrate the effect of mechanical properties on electrical response behavior, a force-electric coupling model was developed using Abaqus finite element simulations.[46] The electric field forces on Agar/PSBMA hydrogels with varying polymer contents were simulated, and the modulus, electric field forces, and displacements of the different hydrogels were recorded (**Figure 8**; Table S3 and Movie S6, Supporting Information). The simulations show that PSBMA has less effect on the modulus of the hydrogels when Agar content is constant, but it increases the electrodynamic driving force, leading to a larger driving displacement. Conversely, increasing Agar content significantly increases the electric field force but requires

the hydrogel to overcome greater internal mechanical stress to bend, reducing the electric driving force and the bending displacement. In summary, the degree of response of a hydrogel actuator is influenced by both its charge movement and polarization under external electric fields and its own mechanical properties, which affect the deformation and responsiveness of the actuator.

3. Conclusion

To solve problems of strict preparation and narrow response range, a versatile Agar-Zwitterion hybrid hydrogel was developed by incorporating PSBMA with strong dipole interactions into a temperature-sensitive Agar matrix. Owing to the unique multiplex complementary structure formed by the preforming post-enhancing and mechanical pressing methods, the hybrid Agar/PSBMA hydrogel exhibited excellent mechanical properties with a maximum tensile strength of 47.3 kPa at a maximum elongation at a break of 812% and maintained the tensile strength at 100% after 50 cycles and adhesion properties to various surfaces. Agar/PSBMA hydrogel can be used as a temperature self-sensing material owing to the UCST temperature provided by PSBMA. The hydrogel actuator exhibits both high-voltage and low-voltage electrical response properties, reaching maximum bending angles of 86° in 1 s and 55° in 30 min, respectively due to the strong dipole–dipole interaction. Additionally, through electrical conductivity, dielectric properties, and Abaqus finite element simulation, it was found that the electrical response behavior is influenced by the polarizability and mechanical properties of the hydrogel. This method paves the path for controllable preparation, and multi-stimuli responses of versatile hydrogel actuators, making it a potential candidate for applications in sensors and soft robotics.

4. Experimental Section

Materials: Agar (ash content ≤ 5.0%; gel strength of 1000–1200 g cm^{-2}), was purchased from Shanghai Aladdin Biochemical Technology Co., Ltd. (China). 3-[N, N″-dimethyl-2-(2-methylprop-2-benzyloxy)ethylammonium]propane-1-sulfonate inner salt (purity 98%) (SBMA), N, N′-methylene bisacrylamide (purity 99%) (MBAA), ammonium persulfate (APS) (purity >99.0%), tetramethylethylenediamine (TEMED) (purity 99%), silicone oil (viscosity 350 mPa s), were all obtained from Shanghai Myriad Chemical Technology Co. Ltd. (China).

Preparation of Agar/PSBMA Hydrogel: Agar/PSBMA hydrogel was prepared using the preforming post-enhancing method. First, a certain amount of Agar and deionized water was heated and stirred to completely dissolve the Agar. Once a certain amount of SBMA was added and completely dissolved in the mixed solution, it was quickly poured into a glass Petri dish to form a preformed hydrogel. Second, the preformed hydrogel was immersed in an MBAA/APS/TEMED mixed solution, sealed, and placed in an oven at 40 °C for 24 h for polymerization. Following this, different forces were pressed onto the hydrogel that had an area of 63.6 cm^2 for 48 h to obtain the post-enhanced and mechanically pressed Agar/PSBMA hydrogel. Agar/PSBMA prepared by 1 wt.% Agar, 0.7 mol L^{-1} SBMA, and pressed by a 630 g weight (pressure of 970 Pa) was used in subsequent experiments unless otherwise stated. The material ratios of the components are shown in Table S1 (Supporting Information).

The hydrogel was prepared by the conventional method for comparison. Specifically, after the Agar and SBMA were dissolved, MBAA/APS/TEMED mixed solution was directly added to the sol, poured into a Petri dish, and polymerized at 40 °C for 24 h, followed by mechanical pressing.

Characterizations: The content of elements in the samples as well as the energy density was analyzed using a PHI Quantera II photoelectron spectrometer (Ulvac-PHI Corporation, Japan). A Bruker Alpha II ATR-FTIR spectrometer (Bruker, Germany) was used to characterize the functional group structure of the sample organics. The cross-sectional morphology of the freeze-dried hydrogel samples was characterized using a Regulus 8230 SEM (Hitachi, Japan) with an operating voltage of 3.0 kV. Rheological performance: A Physica MCR 302 rheometer (Anton Parr, Austria) was used to determine the modulus of the hydrogel samples. The hydrogels were tested for tensile, compression, cyclic compression, and adhesion using an Instron 6022 universal material tester (Instron, USA).

Temperature Self-Sensing: To test the visible detected temperature self-sensing function, transparency, and temperature changes in hydrogel were recorded under heating using a T2L infrared camera (iRay, China). The transmittance of the hydrogels was tested by the Lambda950 UV–vis-NIR Spectrophotometer (PerkinElmer, USA) under different temperatures.

Electrical Response Performance: To test the electrical response performance of hydrogel actuators, a test platform (Movie S4, Supporting Information) was developed, and the response of hydrogel actuators with different components was recorded with a camera when a high voltage of 20 kV or a low voltage electric field of 9–15 V was applied, after which the electrical response rate and bending angle of the hydrogel were analyzed using PicPick software.

Additionally, the conductive and dielectric properties of hydrogels were investigated for the mechanism and factors influencing the electrical response. The electrical conductivity was measured by its AC impedance spectrum with a CHI760E electrochemical workstation (Shanghai Chenhua Instruments Co., Ltd., China). The dielectric constant was tested with a Hantek 183X handheld LCR bridge.

Force-Electric Coupling Analysis: The bending behaviors of Agar/PSBMA hydrogels were simulated by Abaqus software. The force analysis and displacement changes of the hydrogels were used to simulate the mechanism and influencing factors of the bending of the hydrogel actuators under the action of the electric field, and the properties were compared with those of Agar hydrogels and PSBMA hydrogels. The model of the simulated hydrogel was created in the component. The parameters of the mechanical properties of the hydrogel were modified. The boundary conditions were selected in the load. At this point, the hydrogel was subjected to its own gravity and electric field forces. The electric field force was added to the side of the hydrogel in the form of a force field. The magnitude of the electric field force on the hydrogel was determined by simulating the actual bending of the Agar/PSBMA hydrogel. Detailed experimental steps can be found in the Supporting Information.

Statistical Analysis: The data were expressed as mean ± SD of at least three parallel experiments.

Supporting Information

Supporting Information is available from the Wiley Online Library or from the author.

Acknowledgements

J.Y. and W.H. contributed equally to this work. This work was supported by the Beijing Natural Science Foundation (grant no. L222036), Special Key Projects (grant no. 2022-JCJQ-ZD-224-12), and the Chinese Scholarship Council under grant no. 202206030117 and 202206030077. N.-J.C. gratefully acknowledged funding support from the Ministry of Education in Singapore under grant no. MOE-MOET32022-0002.

Conflict of Interest

The authors declare no conflict of interest.

Data Availability Statement

The data that support the findings of this study are available from the corresponding author upon reasonable request.

Keywords

actuators, adhesion, hybrid double-network hydrogels, temperature self-sensing, wide-range electrical response

Received: November 3, 2023
Revised: December 15, 2023
Published online:

[1] H. Liu, H. Luo, J. Huang, Z. Chen, Z. Yu, Y. Lai, *Adv. Funct. Mater.* **2023**, *33*, 2302038.
[2] Z. Zhao, J. Deng, H. Tae, M. S. Ibrahim, S. Suresh, N.-J. Cho, *Adv. Mater.* **2022**, *34*, 2109367.
[3] W. Xu, P. Dong, S. Lin, Z. Kuang, Z. Zhang, S. Wang, F. Ye, L. Cheng, H. Wu, A. Liu, *Sens. Actuators, B* **2022**, *359*, 131547.
[4] J. Simińska-Stanny, M. Nizioł, P. Szymczyk-Ziółkowska, M. Brożyna, A. Junka, A. Shavandi, D. Podstawczyk, *Addit. Manuf.* **2022**, *49*, 102506.
[5] K. Rotjanasuworapong, N. Thummarungsan, W. Lerdwijitjarud, A. Sirivat, *Carbohydr. Polym.* **2020**, *247*, 116709.
[6] A. López-Díaz, A. Martín-Pacheco, A. M. Rodríguez, M. A. Herrero, A. S. Vázquez, E. Vázquez, *Adv. Funct. Mater.* **2020**, *30*, 2004417.
[7] R. K. Cheedarala, J.-H. Jeon, C.-D. Kee, I.-K. Oh, *Adv. Funct. Mater.* **2014**, *24*, 6005.
[8] H. Jiang, L. Fan, S. Yan, F. Li, H. Li, J. Tang, *Nanoscale* **2019**, *11*, 2231.
[9] J. Shang, Z. Shao, X. Chen, *Biomacromolecules* **2008**, *9*, 1208.
[10] P. Xue, C. Valenzuela, S. Ma, X. Zhang, J. Ma, Y. Chen, X. Xu, L. Wang, *Adv. Funct. Mater.* **2023**, *33*, 2214867.
[11] J. Yang, J. Yao, S. Wang, *Carbohydr. Polym.* **2022**, *275*, 118717.
[12] I. Ali, L. Xudong, C. Xiaoqing, J. Zhiwei, M. Pervaiz, Y. Weimin, L. Haoyi, M. Sain, *Mater. Sci. Eng. C* **2019**, *103*, 109852.
[13] Y. Zu, Y. Zhang, X. Zhao, C. Shan, S. Zu, K. Wang, Y. Li, Y. Ge, *Int. J. Biol. Macromol.* **2012**, *50*, 82.
[14] a) Y. Shin, M.-Y. Choi, J. Choi, J.-H. Na, S. Y. Kim, *ACS Appl. Mater. Interfaces* **2021**, *13*, 15633; b) K. Saeaeh, N. Thummarungsan, N. Paradee, P. Choeichom, K. Phasuksom, W. Lerdwijitjarud, A. Sirivat, *Eur. Polym. J.* **2019**, *120*, 109231.
[15] J. Yang, Y. Chen, L. Zhao, J. Zhang, H. Luo, *Polym. Rev.* **2023**, *63*, 574.
[16] Z. Nie, K. Peng, L. Lin, J. Yang, Z. Cheng, Q. Gan, Y. Chen, C. Feng, *Chem. Eng. J.* **2023**, *454*, 139843.
[17] J. Wang, J. Zeng, H. Wu, L. Zeng, S. Xu, *J. Appl. Polym. Sci.* **2023**, *140*, 54499.
[18] H. Ghasemzadeh, S. Afraz, M. Moradi, S. Hassanpour, *Int. J. Biol. Macromol.* **2021**, *179*, 532.
[19] M. R. De Guzman, C. K. A. Andra, M. B. M. Y. Ang, G. V. C. Dizon, A. R. Caparanga, S.-H. Huang, K.-R. Lee, *J. Membr. Sci.* **2021**, *620*, 118881.
[20] Z. Wang, J. Li, L. Jiang, S. Xiao, Y. Liu, J. Luo, *Langmuir* **2019**, *35*, 11452.
[21] H. Lee, E. Puodziukynaite, Y. Zhang, J. C. Stephenson, L. J. Richter, D. A. Fischer, D. M. Delongchamp, T. Emrick, A. L. Briseno, *J. Am. Chem. Soc.* **2015**, *137*, 540.
[22] J. Yang, H. Wang, W. Huang, K. Peng, R. Shi, W. Tian, L. Lin, J. Yuan, W. Yao, X. Ma, Y. Chen, *Mater. Horiz.* **2023**, *10*, 3797.
[23] T. Xiang, T. Lu, W.-F. Zhao, C.-S. Zhao, *Langmuir* **2019**, *35*, 1146.
[24] H. Cui, N. Pan, W. Fan, C. Liu, Y. Li, Y. Xia, K. Sui, *Adv. Funct. Mater.* **2019**, *29*, 1807692.
[25] J. P. Gong, *Soft Matter* **2010**, *6*, 2583.
[26] a) G. Wei, Y. Kudo, T. Matsuda, Z. J. Wang, Q. F. Mu, D. R. King, T. Nakajima, J. P. Gong, *Mater. Horiz.* **2023**, *10*, 4882; b) T. Matsuda, R. Kawakami, R. Namba, T. Nakajima, J. P. Gong, *Science* **2019**, *363*, 504.
[27] Z. Xiao, Q. Li, H. Liu, Q. Zhao, Y. Niu, D. Zhao, *Eur. Polym. J.* **2022**, *173*, 111277.
[28] N. Wang, B. T. Seymour, E. M. Lewoczko, E. W. Kent, M.-L. Chen, J.-H. Wang, B. Zhao, *Polym. Chem.* **2018**, *9*, 5257.
[29] J. Ning, K. Kubota, G. Li, K. Haraguchi, *React. Funct. Polym.* **2013**, *73*, 969.
[30] S. Ge, J. Li, J. Geng, S. Liu, H. Xu, Z. Gu, *Mater. Horiz.* **2021**, *8*, 1189.
[31] L. Bai, Y. Jin, X. Shang, H. Jin, L. Shi, Y. Li, Y. Zhou, *Nano Energy* **2022**, *104*, 107962.
[32] V. Baddam, H. Tenhu, *Polym. Chem.* **2023**, *14*, 3647.
[33] H. Sun, J. Chen, X. Han, H. Liu, *Mater. Sci. Eng. C* **2018**, *82*, 284.
[34] L. Xu, H. Zheng, F. Xue, Q. Ji, C. Qiu, Q. Yan, R. Ding, X. Zhao, Y. Hu, Q. Peng, X. He, *Chem. Eng. J.* **2023**, *463*, 142392.
[35] Z. Liang, S. Jiang, H. Jiang, X. Zhao, B. Jin, G. Chen, S. Lo, *Chem. Eng. J.* **2023**, *451*, 139054.
[36] I. Apsite, S. Salehi, L. Ionov, *Chem. Rev.* **2022**, *122*, 1349.
[37] T. Shiga, T. Kurauchi, *J. Appl. Polym. Sci.* **1990**, *39*, 2305.
[38] W. Mei, A. J. Rothenberger, J. E. Bostwick, J. M. Rinehart, R. J. Hickey, R. H. Colby, *Phys. Rev. Lett.* **2021**, *127*, 228001.
[39] a) L. Chen, X. Wei, Y. Sun, Y. Xue, J. Wang, Q. Wu, C. Ma, X. Yang, G. Duan, F. Wang, S. Jian, W. Yang, S. Jiang, *Chem. Eng. J.* **2022**, *446*, 137072; b) H. Dai, S. Ou, Y. Huang, Z. Liu, H. Huang, *Cellulose* **2018**, *25*, 593.
[40] a) Z. Ying, Q. Wang, J. Xie, B. Li, X. Lin, S. Hui, *J. Mater. Chem. C* **2020**, *8*, 4192; b) Y. Gao, H. Deng, J. Zhang, Q. Shu, Z. Xu, X. Cao, B. Wang, X. Gong, *Adv. Mater. Technol.* **2022**, *7*, 2200047; c) Z. Wang, Y. Wang, Z. Wang, Q. He, C. Li, S. Cai, *ACS Appl. Mater. Interfaces* **2021**, *13*, 24164; d) G. M. Milani, I. T. Coutinho, F. N. Ambrosio, M. H. Monteiro Do Nascimento, C. B. Lombello, E. C. Venancio, M. Champeau, *J. Appl. Polym. Sci.* **2022**, *139*, 52091.
[41] J. Min, D. Barpuzary, H. Ham, G.-C. Kang, M. J. Park, *Acc. Chem. Res.* **2021**, *54*, 4024.
[42] K. Petcharoen, A. Sirivat, *Curr. Appl. Phys.* **2013**, *13*, 1119.
[43] W. Mei, A. Han, R. J. Hickey, R. H. Colby, *J. Chem. Phys.* **2021**, *155*, 0074100.
[44] O. Kim, H. Kim, U. H. Choi, M. J. Park, *Nat. Commun.* **2016**, *7*, 13576.
[45] L. Gharavi, M. Zareinejad, A. Ohadi, *Mechatronics* **2022**, *81*, 102690.
[46] H. Tian, H. Li, Z. Yuan, X. Liu, Y. Li, Y. Qi, P. Ding, *J. Ambient. Intell. Humaniz. Comput.* **2020**, *11*, 6283.